

Effect of Inter-Column Spacing on Soil Stresses due to Vibro-Installed Stone Columns: Interesting Findings

Hesham Elshazly · Mohamed Elkasabgy · Azza Elleboudy

Received: 27 July 2006 / Accepted: 12 November 2007 / Published online: 20 December 2007
© Springer Science+Business Media B.V. 2007

Abstract This paper reveals the interesting relation between the inter-column spacing and the corresponding alteration of soil state of stresses due to the vibro-installation technique. This relation is inferred from analyses for load settlement records of various field load tests, performed for stone columns arrangements with different inter-column spacing values. In order to have adequate confidence in the findings, a well-documented case history, involving three columns patterns along with their relevant field and laboratory test results, is utilized for this study. Moreover, a well-tested finite element model, capable of simulating both elasto-plastic and time dependent soil deformations as well as pore water pressure

building and dissipation, is employed in the analysis. Instead of determining the soil response to the test load, based on known initial soil stresses and material properties, the analysis is inversely posed to determine the soil initial stresses, based on the recorded settlements and the post-installation material properties. The alteration in the soil state of stress is represented by the increase in the post-installation horizontal to vertical stress ratio, K^* , as a function of the inter-column spacing. It is found that this alteration experiences a systematic decrease in its magnitude as the inter-column spacing increases.

Keywords Back analysis · Ground improvement · Stone columns · Soil stresses

H. Elshazly
Department of Soil and Structural Dynamics,
Construction Research Institute, National Water Research
Center, Cairo, Egypt

H. Elshazly (✉)
Dar Al-Handasah (Shair and Partners), Gulf Tower, Oud
Metha Road, P.O. Box 55624, Dubai,
United Arab of Emirates
e-mail: longatthe@yahoo.com

M. Elkasabgy
Department of Civil and Environmental Engineering,
University of Western Ontario, London, ON, Canada

A. Elleboudy
Department of Civil Engineering, Faculty of Engineering,
Banha University, Cairo, Egypt

Notations

a_r	Area replacement ratio
c'	Drained shear strength of cohesive soil
d	Distance between the diagonal column and the reference column
E'	Drained modulus of elasticity
E_{50}^{ref}	Reference stiffness modulus corresponding to the reference confining pressure
K^*	Post-installation coefficient of lateral earth pressure
K_o	At-rest coefficient of lateral earth pressure
K_p	Passive coefficient of lateral earth pressure
K_x	Coefficient of horizontal permeability

K_z	coefficient of vertical permeability
m	The exponent of stress-dependent stiffness
p^{ref}	Reference stress for soil stiffness evaluation ($p^{\text{ref}} = 100 \text{ kN/m}^2$)
R	Column radius
R_f	Failure ratio
S	Spacing between stone columns
ϕ'	Effective angle of internal friction
γ_d	Dry unit weight
γ_{sat}	Saturated unit weight
ν	Drained Poisson's ratio

1 Introduction

Because of the ever-increasing value of land, the development of marginal sites is now economically feasible. The increased cost of conventional foundations, like concrete piles, and their environmental constraints greatly encouraged the improvement of weak soils via natural means. The vibro-stone-columns technique has, therefore, become a vital method of ground improvement and reinforcement. This technique has, generally, been proven successful in increasing the stiffness of weak soils, upgrading their safe bearing capacity, and reducing their total and differential settlements, as well as speeding up their consolidation process. In the current study, however, no preloading was considered and, therefore, the accelerated rate of consolidation is not demonstrated.

The insertion of stone columns into weak soils by vibro-installation technique is not just a replacement operation. This is due to the fact that such installation technique is accompanied by vibration and horizontal displacement of soil. Consequently, it is believed to cause positive changes in both the material properties and the state of stresses in the treated soil mass. Successful analysis of vibro-installed stone column systems, therefore, suggests that these changes be studied and their effect on the treated ground performance be quantified. As a result, more optimized design can be achieved.

Despite the widespread use of stone columns, the stress alteration in the soil mass was scarcely taken into account in both the numerical analysis and the laboratory-model studies. Despite the brilliance of the laboratory experimental works by Juran and

Guermazi (1988), Madhav (1988), Al-Khafaji and Craig (2000), Matsui et al. (2001), and Akdogan and Erol (2001), it was difficult for them to physically simulate both the radial displacement and the densification effects in their laboratories. They, therefore, adopted the pre-boring method of installation.

It has to be noted that the negligence of radial stress changes in the settlement prediction analysis will overestimate the corresponding field settlements and underestimate the real ultimate capacity of stone columns (Elkasabgy 2005). Kirsch and Sondermann (2001) and Watts et al. (2001) reported that the type of vibro-process has a great effect on both the state of stresses and densification of soil surrounding stone columns. Watts et al. (2001), however, did not provide quantification for the coefficient of lateral earth pressure, K^* , after columns installation. In the wet method, a hole is first formed and during its formation flushing out of soil occurs. The amount of displacement, which causes the consolidation and lateral stress increase in the surrounding soil mass, in this case, depends on the amplitude of vibration of the adopted poker. In the dry method, contrariwise, more displacement occurs during the insertion of the poker itself and the native soil is not flushed out. This displacement is superimposed on the effect of the poker vibration.

Earlier investigations also did not present quantification for the effect of the inter-column spacing on the post-installation soil state of stress. It is, however, believed that differences must occur in the K^* values of reinforced grounds depending on their inter-column spacing.

The question, therefore, was: how significant would the variation of K^* with the inter-column spacing be? It was found interesting and rather challenging for the current authors to find an answer for this essential question. The inverse analysis of real load-settlement records, is believed to be the appropriate strategy to estimate the post-installation alteration in the soil state of stresses, as reflected by the difference between the at-rest coefficient of lateral earth pressure K_0 and the corresponding post-installation value K^* .

By the inverse approach, as opposed to the conventional (forward) analysis approach, load-settlement records from full-scale field tests, each was carried out on a single stone column surrounded by an extended group of similar columns, were analyzed.

In this analysis, instead of determining the soil displacement response to the test load based on known initial soil stresses and material properties, the analysis is inversely posed to determine the soil initial stresses based on knowledge about the system settlements and the post-installation material properties. There is, however, more than one way to perform this back calculation. These, generally, are the formal probabilistic and statistical approaches as well as the simple iterative approach.

The formal inverse analysis tools such as recursive least squares and the Kalman filter provide fully automated mathematical back calculations based on statistical and probabilistic criteria. Despite the freedom of these tools to systematically search for the target solution, they, in many cases, are subject to divergence due to the nature of their mathematical formulation. As demonstrated by Elshazly et al. (1997a, b), introducing simplifications, which lead to better mathematical posedness of this class of problems, has increasingly become a hot issue in this research area.

For problems with considerably large number of degrees of freedom and relatively small number of observation points, it is hard to hope solution by the formal inverse tools. The current study, therefore, appeals to the iterative approach. In the implementation of this approach, a number of rounds of analyses with various reasonable values of K^* were performed. In each round, the chosen value of K^* is fixed and the corresponding settlement is computed. The K^* value that achieves the best match between the simulation and the field test load-settlement curve is considered to represent the post-installation horizontal to vertical stress ratio.

In this paper, the set up and procedure of the field load tests, for the three stone columns patterns, 1.20×1.50 , 1.75×1.75 and 2.10×2.10 m, are first described. Second, the site conditions and the geometrical idealizations for the numerical simulation are illustrated. Third, the soil material testing and modeling are highlighted. Fourth, the evidence for the vibro-installation alteration for the state of stresses in the soil mass is demonstrated. Finally, different strategies, based on varying the confidence level in the used post-installation soil parameters, are introduced to identify a best estimate for K^* as well as a possible practical range for the value it may assume in the three analyzed cases.

2 Site Characteristics at Field Load Tests Location

As mentioned above, records from field load tests on individual stone columns, located within extended groups of similar columns, were utilized to back calculate the horizontal to vertical soil stress ratio K^* for stone columns arrangements with different inter-column spacing values. The adopted load tests were selected from 28 load tests carried out for a large wastewater treatment plant founded in California, USA. In the selection, and in order to obtain a reliable conclusion, the authors tried to pick up the tests carried out on columns arrangements with different spacing values, covering the practical range from 1.20 to 2.10 m.

The loading criterion for the field load procedure was such that an increment of load is added when the rate of settlement decreased to 0.25 mm/h. For further details on the load tests, reference can be made to Mitchell and Huber (1985).

The soil profile typically comprises estuarine deposits underlain by older marine deposits. The thickness of the soft estuarine deposits beneath the structural foundation grade was found in average to be 10.80 m approximately. The total depth of the older marine sediments is unknown, but, it was suggested from geological evidence that it might extend to as deep as 600 m beneath the ground surface. Ground water level occurs within 1.50 m from the ground surface. A typical soil profile for the upper 15 m of the site soils is shown in Fig. 1.

Over 6,500 stone columns were installed by the wet vibro-replacement method. The columns installation started with jetting a T-Type vibrator, 290 mm in diameter, down to the desired depth with water. It, therefore, added approximately 100 mm of annular space supported by water pressure. Then, the formed hole was filled in stages with well-graded gravel and each stage was thoroughly compacted by the reinsertion of the vibrator, pushing the gravel laterally against soil. All stone columns extended completely through the soft estuarine deposits and penetrated about 0.30 m into the older marine deposits. They were arranged in square and rectangular patterns. The curves of applied pressure versus settlement, obtained from loading tests on columns within three different stone column spacing patterns, 1.20×1.50 , 1.75×1.75 , and 2.10×2.10 m, are shown in Fig. 2. The corresponding tributary areas of the aforementioned patterns are

Fig. 1 Typical site soil profile

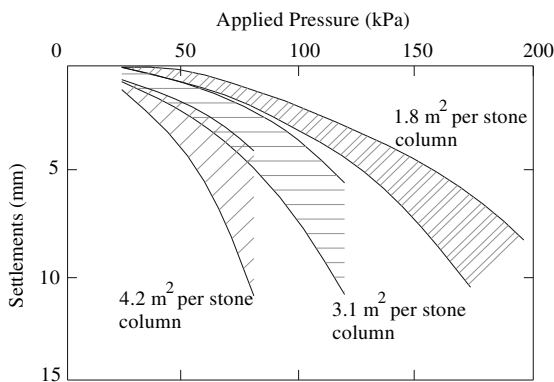
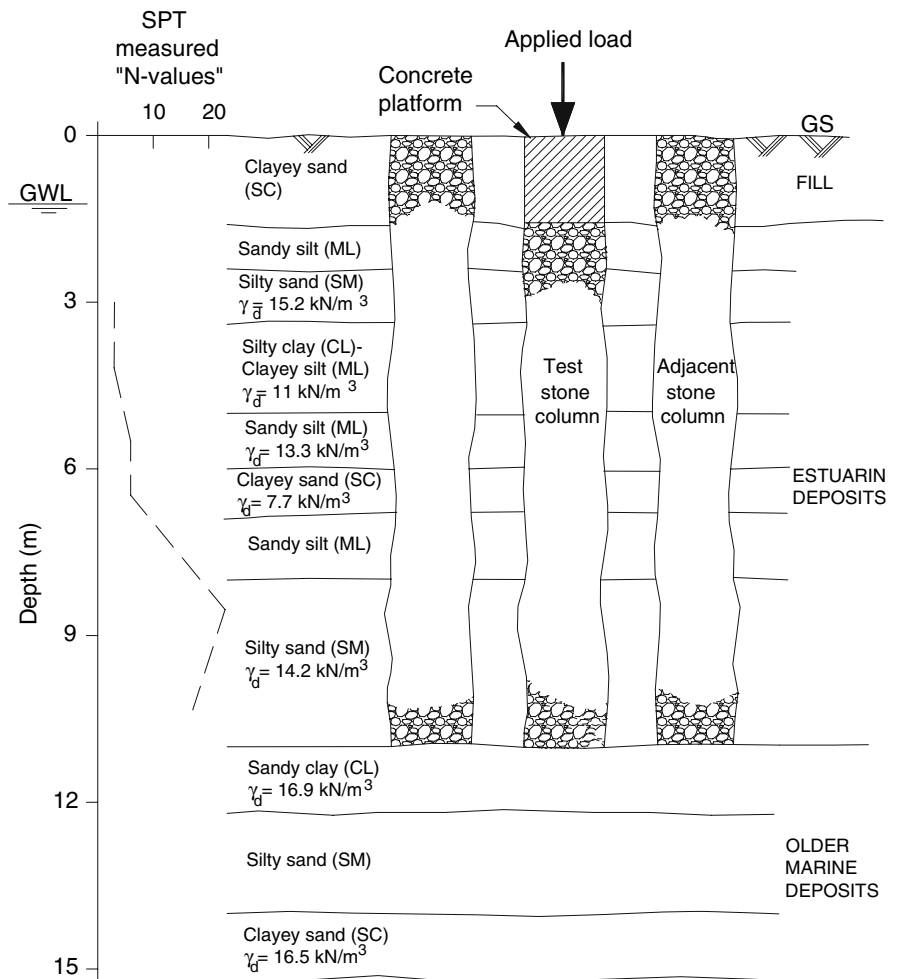


Fig. 2 Ranges of load-settlement curves for different stone column patterns

1.80, 3.10, and 4.20 m², respectively. The variations observed in the range of load-settlement curves corresponding to a given pattern can be attributed

mainly to the non-uniformity of the soil properties in the estuarine deposits and the variable depth to the older marine deposit.

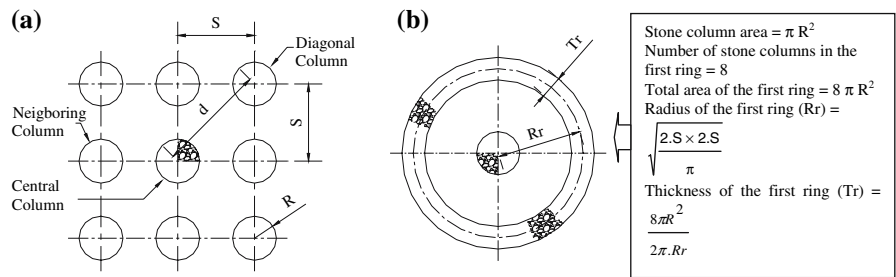
The load test procedure was in accordance with the requirements of the test method ASTM D1194-66, with the only exception that the standard 0.762 m steel plate was replaced with a 2.0 m diameter circular concrete slab located concentrically over the test stone column. The load was applied in increments, and the loading criterion was such that no load increment was added before the rate of settlement was less than 0.25 mm/h.

3 Mathematical Simulation

3.1 Geometric Modeling

The arrangement of the test columns is generally 3D. Their large extent property, however, suggests that

Fig. 3 Idealization of concentric rings: (a) stone columns grid with respect to a reference column; and (b) calculation of concentric ring dimensions (after Elkasabgy 2005)



the axisymmetrical idealization is an appropriate geometrical simulation. In this model, the test column is set at the center of successive concentric rings having their centers coincident with the center of this column. The dimensions of the concentric rings were chosen such that the area replacement ratio, defined as the ratio of stone columns area to the total area, in the model equals the corresponding one in the field. The idealization of the first concentric ring for the model is depicted by Fig. 3. The analyzed patterns, 1.20×1.50 , 1.75×1.75 , and 2.10×2.10 m, have the geometrical parameters and maximum applied stresses shown in Table 1.

Similar modeling strategy was adopted by Mitchell and Huber (1985) and Elshazly et al. (2006). Nevertheless, further refinements to the geometrical model were applied in the current study, aiming at enhancing the outcome of the simulation. In the earlier studies, the spacing between successive rings was taken equal to the spacings, between adjacent columns. This condition, however, results in overestimating the stiffness contribution of the diagonal columns, which are more distant from the central column than the orthogonally arranged ones, as apparent from Fig. 3a. In the present investigation, the spacing between the concentric rings is adjusted to account for the difference between the distance, d , of a diagonal column, and the corresponding distance, S , of an orthogonal column. This version of the geometrical model is therefore believed to achieve

better confidence in the obtained results. The idealization formulae for the first concentric ring are given in Fig. 3.

The soil profile was the same as that adopted by Mitchell and Huber (1985). However, use was made of more accurate modeling by utilizing a finer mesh of 15-node triangular elements. The typical axisymmetrical finite element mesh used to simulate the individual load tests is depicted by Fig. 4. The shown arrangement and spacing values are pertinent to the stone column pattern 1.75×1.75 m. In the model, the rigid horizontal boundary was imposed at a depth of 19.2 m.

3.2 Material Modeling

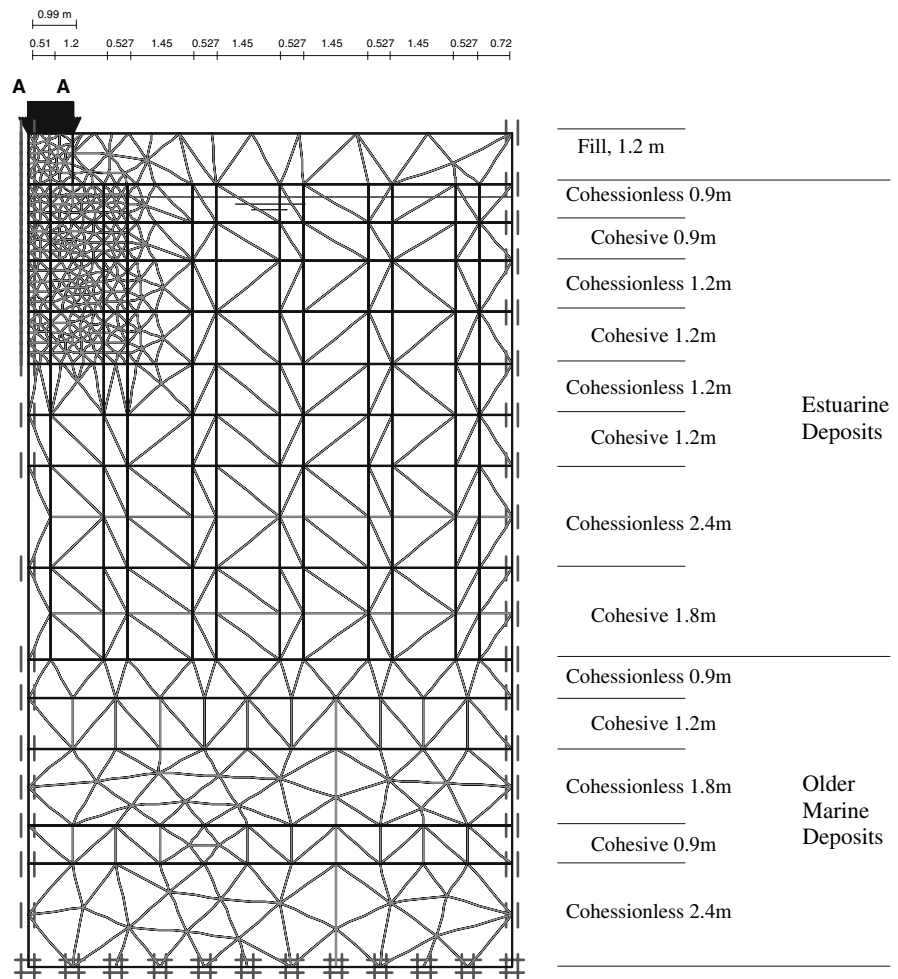
The hyperbolic hardening soil model, originally developed by Duncan and Chang (1970), incorporated with modifications that lead to successful simulation of the unloading–reloading stress reversals, was adopted for the four types of the site soil (Fig. 4), namely: the estuarine cohesive, the estuarine cohesionless, the marine cohesive and the marine cohesionless soils, as well as the gravel that forms the installed stone columns. At failure stresses, the adopted model satisfies the Mohr–Coulomb failure criterion. The time dependent (water-solids) coupled model, incorporated with the employed code, enables the simulation of both the excess pore water pressure and the settlement rate criterion set for the test. This coupled finite element formulation employs drained soil parameters for both cohesive and cohesionless soils.

The material parameters of the four types of the site soil and the gravel material in the stone columns were determined from averaging the results of several tests performed on each soil (Mitchell and Huber 1985). The tested samples were taken after the

Table 1 Geometry and loading for the analyzed columns

Columns pattern (m)	Column diameter (m)	Column length (m)	Area replacement ratio (a_r) (%)	Maximum applied stress (kPa)
1.20×1.50	0.96	12.35	40.20	170
1.75×1.75	1.02	11.13	26.67	120
2.10×2.10	1.06	11.40	21.00	81

Fig. 4 Geometry and finite element mesh for columns pattern 1.75×1.75 m



installation of stone columns. They, therefore, readily account for the improvement in soil properties during the installation of stone columns. The remaining unknown to be determined by back analysis is the alteration in the soil state of stress.

In the first round of analysis, the hardening model soil parameters, presented in Table 2, were adopted (PLAXIS, version 7; 1998). These parameters are the drained cohesion c' , the drained angle of shearing resistance ϕ' , the dry and saturated unit weights γ_d and γ_{sat} , the failure ratio R_f , the reference stiffness modulus E_{50}^{ref} and the exponent of stress-dependent stiffness m , which reflects the confining pressure dependency of E_{50}^{ref} .

The elastic-perfectly plastic stress–strain relationship incorporated with Mohr–Coulomb failure criterion was utilized to simulate the properties of the concrete platform and the fill layer (Table 3). The approximation of the at-rest horizontal to vertical

stress ratio, $K_o = 0.5$, which was assumed by Mitchell and Huber (1985) for the marine deposits, is believed to be reasonable, and is, therefore, adopted in the present study.

In order to model the dissipation of the excess pore water pressure, generated during the test loading, reasonable values for the coefficient of permeability for the site soils need to be estimated. It is believed that the use of very high permeability coefficient values for both stone column material and cohesionless soils is not reasonable. This is attributed to the infiltration of silt and clay particles into the granular material of the stone columns during installation, and the presence of considerable percentage of these fine materials even in the cohesionless layers. The intrusion of these fines into the stone columns reduces the effectiveness of water drainage in the radial direction. A permeability coefficient value of $K_z = 10^{-5}$ m/s for

Table 2 Adopted soil parameters

Soil classification	Estuarine cohesive	Estuarine cohesionless	Marine cohesive	Marine cohesionless	Gravel
Model	Hardening model	Hardening model	Hardening model	Hardening model	Hardening model
Behavior	Undrained	Drained	Undrained	Drained	Drained
γ_d (kN/m ³)	15	15	17	17	18.60
γ_{sat} (kN/m ³)	19	19	20	20	21.60
C' (kPa)	0	0	0	0	0
ϕ' (°)	34	38	34	37	41
E_{50}^{ref} (kPa)	8500	17,000	8700	12,600	29,200
m	0.65	0.69	0.65	0.90	0.59
P^{ref} (kPa)	100	100	100	100	100
R_f	0.87	0.69	0.67	0.67	0.86
K_z (m/s)	1×10^{-8}	1×10^{-6}	1×10^{-8}	1×10^{-6}	1×10^{-5}
K_x (m/s)	2×10^{-8}	2×10^{-6}	2×10^{-8}	2×10^{-6}	2×10^{-5}

the stone column material (gravel), and a value of $K_z = 10^{-6}$ m/s for the cohesionless layers were, therefore, adopted in the current investigation (Lambe and Whitman 1979; Todd 1980; Francis 1985; Craig 1992; Powers 1992; Donald 1999).

The site cohesive soils contained an appreciable percentage of silt and sand, and had relatively low liquid limits. Lambe and Whitman (1979) and Francis (1985) noted that for low liquid limit silts and clays, the permeability coefficient value varies between 10^{-7} and 10^{-8} m/s. Based on their range, a value of 10^{-8} m/s can reasonably be assigned for such soils. As for the relation between the vertical, K_z , and the horizontal, K_x , coefficients of permeability, Lambe and Whitman (1979) reported that a value for the horizontal to vertical permeability ratio, of 2–10, is not unusual in normally consolidated sedimentary clay.

Table 3 Fill and concrete parameters

Material	Fill	Concrete
Model	Elastic-perfectly plastic	Elastic-perfectly plastic
Behavior	Drained	Non porous
γ_d (kN/m ³)	16	25
γ_{sat} (kN/m ³)	19	–
c' (kPa)	0	4000
ϕ' (°)	30	40
E' (kPa)	10,000	2×10^7
ν	0.33	0.15
K_z (m/s)	1×10^{-6}	0
K_x (m/s)	2×10^{-6}	0

It was observed from several trials, with different vertical to horizontal permeability ratios, that the resulting settlements were insensitive to the variation in the relation between vertical and horizontal permeability coefficients. This is attributed to the nearly full dissipation of excess pore water pressures during tests, due to the small vertical and radial drainage paths through the soil-stone column system. This behavior underlines the advantageous drainage property of the stone columns, as reported by Barksdale and Bachus (1983), Han and Ye (1993, 2001) and Watts et al. (2001). Based on the above findings and discussion, a ratio of $K_x = 2K_z$ was adopted for all types of soils in the model.

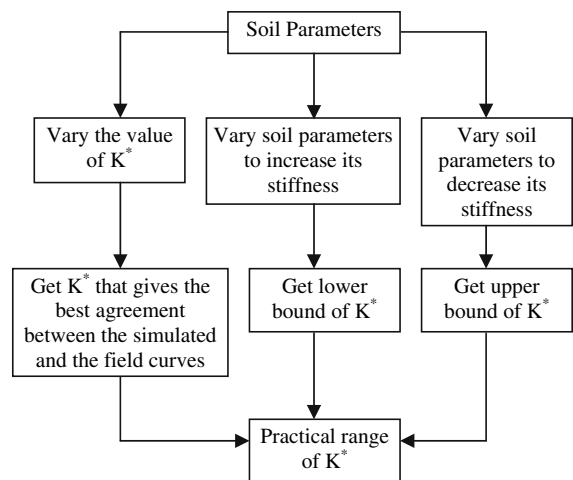


Fig. 5 Flow chart for K^* evaluation

4 Evaluation of K^* by Back Analysis

To estimate the value of K^* , the methodology illustrated by the flow chart shown in Fig. 5 was adopted. Two strategies were followed to arrive at a reliable quantification of K^* . In the first strategy, full confidence was put in the values of the available laboratory-determined soil parameters, and the corresponding value of K^* was back calculated based on the best match between the model and the field test results. In the second strategy, upper and lower bound values of K^* were back calculated by considering some level of uncertainty in the laboratory-determined soil parameters.

4.1 First Strategy

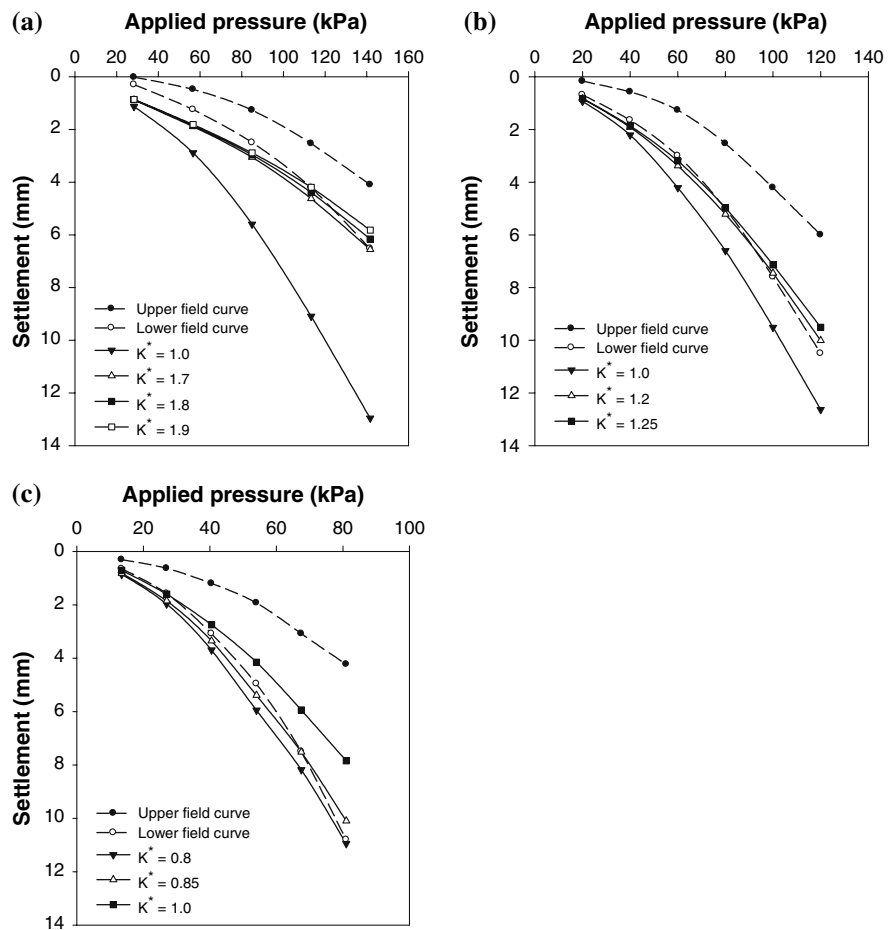
In the first strategy, the parameters given in Table 2 were adopted. The reliability of these parameters

stems from the fact that they were obtained by averaging several well-controlled triaxial tests. In addition, these parameters reflect relatively high stiffness for the given deposits, so they are supposed to cause no exaggeration or over-estimation of the back calculated K^* values. For these reasons, the obtained values of K^* , for the three analyzed patterns, are believed to be the *best conservative* estimates.

For the three analyzed patterns, the lowest value in the previously denoted range of permeability coefficient values for the cohesive strata, $K_z = 1 \times 10^{-8}$ m/s, was chosen, and the value of K^* was varied; each round of the analyses had a different K^* value and resulted in a single curve among those presented in Fig. 6. For each pattern of stone columns, the value of K^* relevant to the curve which achieves the best match with the corresponding field load-settlement curve is deemed to be the best K^* estimate.

The examination of Fig. 6 reveals that the best estimates for K^* are 1.70, 1.20 and 0.85 for the

Fig. 6 Field and simulated settlement curves for various K^* values: (a) 1.2×1.5 m; (b) 1.75×1.75 m; and (c) 2.1×2.1 m



column patterns 1.20×1.50 , 1.75×1.75 , and 2.10×2.10 m, respectively. It is obvious that for the estuarine deposits, these post-installation values are significantly larger than the at-rest values of 0.38 and 0.44 for the cohesionless and the cohesive deposits, respectively, as evaluated from Jacky’s formula. These findings underline the positive effect of the vibro-installation technique on the state of stresses in soil.

4.2 Second Strategy

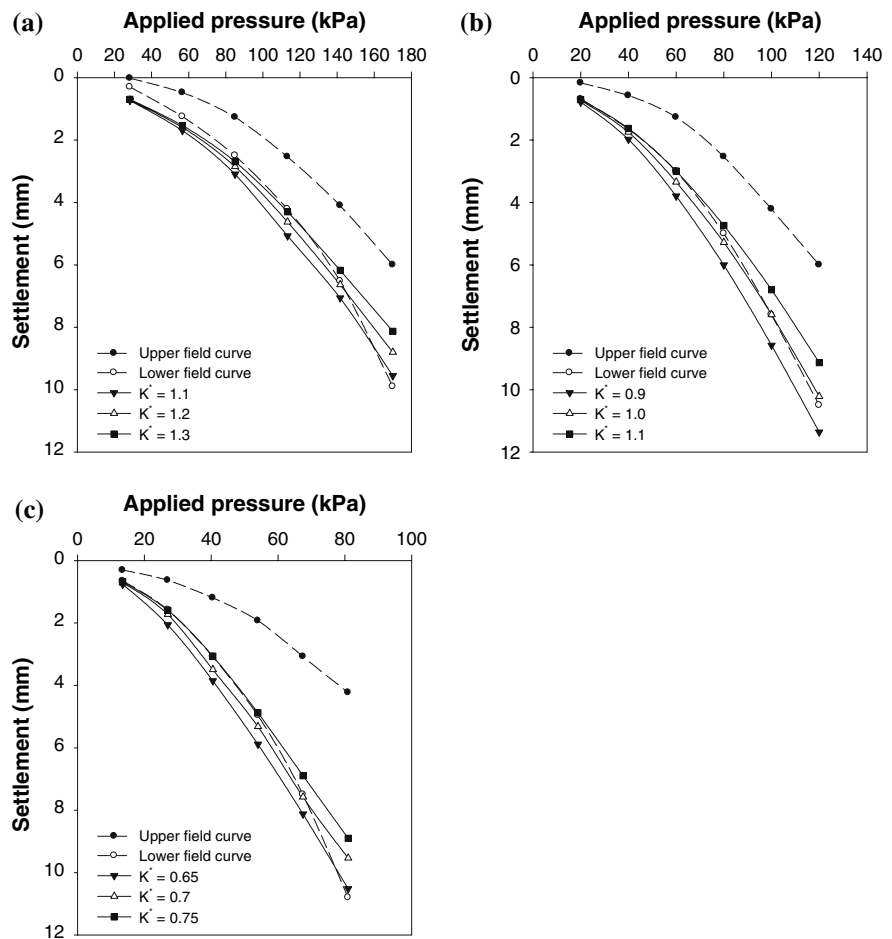
In order to consider the possible uncertainty in the available soil parameters and to further account for any random errors in the analysis, the values of the soil parameters were altered up and down, by reasonable percentages, from their reference values to obtain the corresponding upper and lower bounds of K^* .

The lower bounds of K^* were determined by altering the model parameters in the direction that stiffens the site soils. This, consequently, decreases the system settlements and results in a reduced estimate of the K^* value. The modified model parameters, to simulate a stiffer soil composite, were the reference stiffness modulus E_{50}^{ref} , the angle of internal friction ϕ' , the failure ratio R_f , and the exponent m .

For the largest area replacement ratio, or alternatively the smallest inter-column spacing of 1.20×1.50 m, the stiffness modulus of column material and estuarine deposits were increased by 25% and the angle of internal friction by 3° . For marine deposits, however, E_{50}^{ref} is increased only by 10% and ϕ' by 1° , as it was much less affected by the vibro-installation operation. For the remaining two patterns, 1.75×1.75 m and 2.10×2.10 m, the value of E_{50}^{ref} was increased by 10% and ϕ' by 1° .

The failure ratio R_f and the stress exponent m were decreased to their minimum practical value of 0.5, to

Fig. 7 Field and simulated settlement curves for lower bound estimation of K^* : (a) Columns pattern 1.2×1.5 m; (b) columns pattern 1.75×1.75 m; and (c) columns pattern 2.1×2.1 m



increase the stiffness of all soil layers. The fact that the average confining pressure σ_3 , throughout the most affected soil mass is less than the normalization pressure P^{ref} , which is equal to the atmospheric pressure, causes the global system stiffness to increase as m decreases.

The results of the numerical analyses are illustrated in Fig. 7. The lower bounds of K^* are approximately 1.20, 1.0, 0.70 for column patterns 1.20×1.50 , 1.75×1.75 , and 2.10×2.10 m, respectively. Despite the significant magnification of stiffness, the resulted values of K^* are still higher than the corresponding Jacky's K_o values.

The highest realistic K^* values, the upper bounds for the three analyzed cases, were estimated by altering the soil parameters in the direction that reduces the soil stiffness. The values of E_{50}^{ref} and ϕ' of all modeled soil types in the analyzed column patterns were decreased by 10% and 1° , respectively.

The failure ratio R_f and the stress exponent m were raised to their highest practical values, 0.9 and 1.0, respectively. Based on these parameters, the estimated upper bounds of K^* are 2.0, 1.5, and 1.1 for the 1.20×1.50 , 1.75×1.75 and 2.10×2.10 m column patterns, respectively (Fig. 8).

The numerical model revealed that all the reached values of K^* were larger than the corresponding at-rest values of K_o , but smaller than the ultimate resistance values of K_p . They were also found to compare favorably with the values reported in the literature by other investigators (Table 4). It has to be noted that the difference in the column spacing values for the three analyzed patterns is significant as compared to that in the column diameter values. The columns may, therefore, be considered to have an average diameter of 1.0 m. Thus, the revealed variation in K^* can reasonably be attributed to the corresponding difference in the inter-column spacing

Fig. 8 Field and simulated settlement curves for upper bound estimation of K^* : (a) Columns pattern 1.2×1.5 m; (b) columns pattern 1.75×1.75 m; and (c) columns pattern 2.1×2.1 m

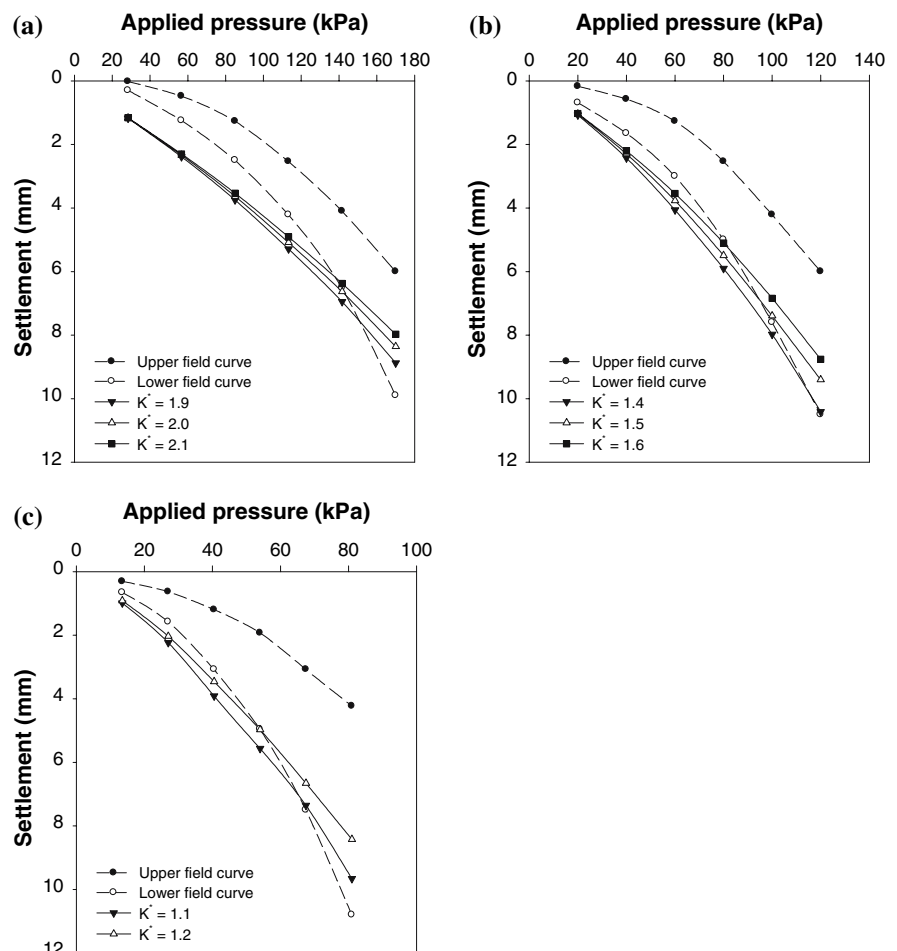


Table 4 Published K^* values versus present investigation

References	K^* value
Elshazly et al. (2006)	Between 1.1 and 2.5, with average of 1.5
Pitt et al. (2003)	Between 0.4 and 2.2, with average of 1.2
Watts et al. (2000)	Between K_o and K_p
Priebe (1995)	1.0
Goughnour (1983)	Between K_o and $1/K_o$
Present study	Between 0.7 and 2.0, with average of 1.2

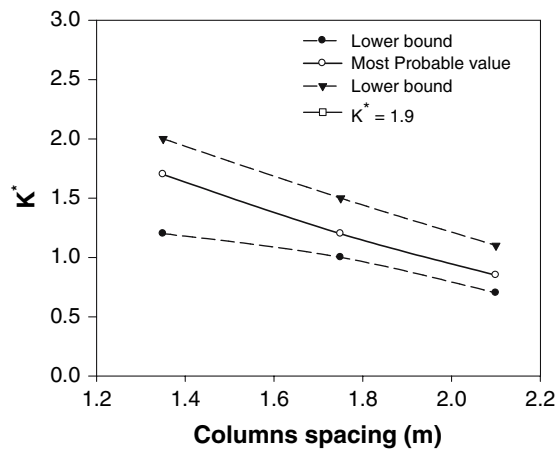


Fig. 9 Variation of K^* with columns spacing

values. Figure 9 depicts the declining trend of K^* with the increase of inter-column spacing. Similar conclusion was reported by Van Impe et al. (1997). They, however, did not quantify the variation of K^* .

5 Conclusions

The relation between the inter-column spacing and the corresponding alteration of soil state of stresses, due to the vibro-installation technique, was investigated. A well-documented case history, involving three columns’ patterns along with their relevant field and laboratory test results, was utilized for this study. Moreover, a well-tested-coupled finite element model, capable of simulating both elasto-plastic and time dependent soil deformations was employed in the analysis. The analysis is inversely posed to

determine the soil initial stresses, based on the recorded settlements and the post-installation material properties. The alteration in the soil state of stress is represented by the increase in the post-installation horizontal to vertical stress ratio, K^* , as a function of the inter-column spacing. The following conclusions are drawn from the investigation:

1. The estimated range of K^* values was from 0.7 to 2.0, with an average of 1.2. The resulted values of K^* underlines the effect of columns installation by the vibro-replacement method on the coefficient of earth pressure K_o .
2. It was found that the post-installation coefficient K^* has values that fits in the range between the at-rest coefficient K_o and the ultimate coefficient K_p .
3. The results of the numerical model revealed the significant role of inter-column spacing on the reinforcing effect of stone columns and indicated the changes anticipated to occur in the soil state of stresses.
4. The values of K^* obtained by back analyzing load settlement records from the field load tests are in harmony with, but rather more conservative than, those obtained by the cavity expansion solution in a separate study (Elkasabgy 2005).
5. The obtained values of K^* in this study are not uniquely corresponding to their respective spacing values. The reason for this is that the K^* values depend, besides the spacing value, on other various factors. Among these factors are the type of installation equipment, its power and its effective amplitude, as well as the soil type and the adopted installation procedure. In the analyzed case history, the vibro-replacement (wet) method was adopted to install the stone columns. The obtained K^* values can, at best, be used as a guide to engineers to realize an optimum design of similar composite systems. Facility of project-dependent judgment is still, however, needed. Further trials are also needed to investigate the K^* values for different other soil conditions and equipment characteristics.

Acknowledgements The authors would like to express their appreciation to Prof. M. R. Madhav from the Indian Institute of Technology for his valuable suggestions. In addition, the authors wish to thank Keller Grundbau Company, Germany, for providing the required data about the project.

References

- Akdogan M, Erol O (2001) Settlement behavior of a model footing on floating sand columns. In: Proc., 5th Int. Conf. on Soil Mech. and Found. Eng., Istanbul, pp 1669–1673
- Al-Khafaji ZA, Craig WH (2000) Drainage and reinforcement of soft clay tank foundation by sand columns. *Géotechnique* 50(6):709–713
- Barksdale RD, Bachus RC (1983) Design and construction of stone columns. Fedral Highway Administration, RD-83/026
- Craig RF (1992) Soil mechanics. Chapman and Hall, London
- Donald PC (1999) Geotechnical engineering: principles and practices, 1st edn. Prentice-Hall, Inc, New Jersey
- Duncan JM, Chang CY (1970) Nonlinear analysis of stress strain in soils. *J Soil Mech Found Div ASCE* 96(SM5):1629–1653
- Elkasabgy MA (2005) Performance of stone columns reinforced grounds. M.Sc. Thesis, Zagazig University, Faculty of Engineering at Shobra, Egypt
- Elshazly HA, Hasegawa T, Murakami A (1997a) An engineering identification method for curvilinear hysteretic systems excited by varying amplitude dynamic loading. *Inverse Probl Eng* 4:177–208
- Elshazly HA, Hasegawa T, Murakami A (1997b) Response prediction of earth structures to future earthquakes based on nonlinear system identification by the VAI method. *Inverse Probl Eng* 5:113–144
- Elshazly HA, Hafez D, Mosaad M (2006) Back calculating vibro-installation stresses in stone columns reinforced grounds. *J Ground Improve* 10(2):47–53
- Francis FD (1985) Soil and rock hydraulics fundamentals. In: Numerical methods and techniques of electrical analogs. A.A. Balkema, Rotterdam, Boston
- Goughnour RR (1983) Settlement of vertical loaded stone columns in soft ground. In: Proc., 8th Europ. Conf. on Soil Mech. and Found. Eng., Helsinki, pp 23–25
- Han J, Ye SL (1993) Field study of an oil tank on stone column ground. In: Proc., 3rd Int. Conf. on Case Histories in Geotech. Eng., St. Louis, Missouri, N. 7.41, pp 1113–1118
- Han J, Ye SL (2001) Simplified method for consolidation rate of stone column reinforced foundations. *J Geotech Geoenviron Eng ASCE* 127(7):597–603
- Juran I, Guermazi A (1988) Settlement response of soft soils reinforced by compacted sand columns. *J Geotech Geoenviron Eng ASCE* 114(8):903–943
- Kirsch F, Sondermann W (2001) Ground improvement and its numerical analysis. In: Proc., 15th Int. Conf. on Soil Mech. and Found. Eng., Istanbul, pp 1775–1778
- Lambe TW, Whitman RV (1979) Soil mechanics. John Wiley & Sons, Inc., SI Version
- Madhav MR (1988) Effect of installation methods on granular pile response. In: Proc., Int. Symp. on Theory and Practice of Earth Reinforcement, I. S., Kyushu, Japan, pp 221–226
- Matsui T, Oda K, Nabeshina Y (2001) Non-linear mechanism and performance of clay-sand column system. In: Proc., 15th Int. Conf. on Soil Mech. and Found. Eng., Istanbul, pp 1803–1806
- Mitchell JK, Huber TR (1985) Performance of a stone column foundation. *J Geotech Eng ASCE* 111(2):205–223
- Pitt JM, White DJ, Gaul A, Hoevelkamp K (2003) Highway applications for rammed aggregate piers in Iowa soils. Iowa DOT Project TR-443, CTRE Project 00-60, USA
- PLAXIS, Version 7 (1998) Finite element code for soil and rock analyses. A.A. Blkema, Rotterdam, The Netherlands
- Powers JP (1992) Construction dewatering: new methods and applications, 2nd edn. John Wiley & Sons, Inc
- Priebe HJ (1995) The design of vibro replacement. *Ground Eng* 28(10):31–37
- Todd DK (1980) Groundwater hydrology, 2nd edn. John Wiley & Sons, Inc
- Van Impe WF, Madhav MR, Vandercruyssen JP (1997) Considerations in stone column design. In: Proc., 3rd Int. Conf. on Ground Improvement Geosystems, London
- Watts KS, Johnson D, Wood LA, Saadi A (2000) An instrumental trial of vibro ground treatment supporting strip foundations in a variable fill. *Géotechnique* 50(6):699–708
- Watts KS, Chown RC, Serridge CJ, Crilly MS (2001) Vibro stone columns in soft clay soil: a trial to study the influence of column installation on foundation performance. In: Proc., 15th Int. conf. on Soil Mech. and Found. Eng., Istanbul, pp 1867–1870